



City Research Online

City, University of London Institutional Repository

Citation: Reyes-Aldasoro, C. C., Biram, D., Tozer, G. M. & Kanthou, C. (2008). Measuring cellular migration with image processing. *Electronics Letters*, 44(13), pp. 791-793.

This is the accepted version of the paper.

This version of the publication may differ from the final published version.

Permanent repository link: <https://openaccess.city.ac.uk/id/eprint/4311/>

Link to published version:

Copyright: City Research Online aims to make research outputs of City, University of London available to a wider audience. Copyright and Moral Rights remain with the author(s) and/or copyright holders. URLs from City Research Online may be freely distributed and linked to.

Reuse: Copies of full items can be used for personal research or study, educational, or not-for-profit purposes without prior permission or charge. Provided that the authors, title and full bibliographic details are credited, a hyperlink and/or URL is given for the original metadata page and the content is not changed in any way.

Measuring cellular migration with image processing

Constantino Carlos Reyes-Aldasoro, Dawn Biram, Gillian M Tozer and Chryso Kanthou

Cancer Research UK Tumour Microcirculation Group, Academic Unit of Surgical Oncology. The University of Sheffield, K Floor, School of Medicine & Biomedical Sciences, Beech Hill Road, Sheffield S10 2RX, U.K.

c.reyes@sheffield.ac.uk

Abstract: An image-processing algorithm for the analysis of migration of vascular endothelial cells in culture is presented. The algorithm correctly detected the cellular regions on either side of an artificial 'wound' made by dragging a sterile pipette tip across the monolayer of cells (scratch wound assay). Frequency filtering and mathematical morphology were used to approximate the boundaries of cellular regions. This allowed the measurement of the distance between the regions, and therefore the migration rates, regardless of the orientation of the wound and even in cases where the cells were sparse and not tightly packed.

Introduction:

The importance of analysing cellular migration *in vitro* relies in the assumption that the dynamic behaviour of cells *in vitro* is related to *in vivo* processes such as wound healing [1] or the activity of metastatic tumour cells [2]. A simple and inexpensive method to study *in vitro* cell migration is with scratch wound assays which consist of a uniform layer of cells where an artificial 'wound' is made by dragging a sterile sharp object such as a needle or micropipette [3]

or through electroporation with an electrical current [4]. Yet, despite the wide use of these scratch wound assays, most of the analysis are limited to the visual observation of a series of microphotographs [2], measurements are generally performed manually, and in the few cases where image processing is used, it requires the images to have a high density of cells [5], well defined borders [6], vertically-oriented straight boundaries [7], or a second fluorescent image [8, 9]. This work presents a robust algorithm to measure the distances between the boundaries that define the edges of a monolayer of migrating vascular endothelial cells in the scratch wound assay. The algorithm uses frequency filtering and mathematical morphology to define an estimate of the boundaries of the cells even in cases with few and sparse cells and there is no user intervention.

Algorithm:

The segmentation algorithm consisted of the following steps: frequency filtering and thresholding, morphological operations, approximation of boundaries and calculation of distances. First, the image was high pass filtered in the Fourier domain to remove the slowly varying intensity inhomogeneities, then a Local Energy Function (low pass filter) was applied. A suitable threshold to segment cells from background was crucial, so the histograms of *quad trees* (QT) [10] of different levels (3-6) were obtained. QT were formed by averaging the intensities of 4 neighbouring pixels of a lower level into the intensity of a new pixel at a higher level of the QT. The effect of the QT was to concentrate the intensity of different classes, at the expense of the spatial resolution. The threshold for each level of the QT was calculated with Otsu's method [11] and the minimum was selected to produce a binary

image. Since there were posterior steps to deal with noise, it was preferred to use a lower level for thresholding, which would capture some noise, than a higher value that would miss some cells.

Next, a series of morphological operators were applied to consolidate the regions. Mathematical morphology [12] considers binary images as point sets. For example, a binary image with a series of black and white pixels can be described as an image I or as a set containing the positions of the white (or the black) pixels: $X=\{(0,0),(1,2),(4,3), \dots\}$. When point set X is combined with another point set B , usually small and known as the structuring element or kernel, a morphological transformation is performed. The two basic morphological operators are *erosion* (also known as shrinking or reducing) and *dilation* (also known as growing, filling or expanding), which erode or enlarge the boundaries of the binary objects contained in the image to which the operator is being applied. Erosion ($X \ominus B$) and dilation ($X \oplus B$) cannot be reversed. Dilation followed by erosion is called *closing* ($X \bullet B = (X \ominus B) \oplus B$) and the opposite, erosion followed by dilation, is called *opening* ($X \circ B = (X \oplus B) \ominus B$). To generate an optimal structuring element, the orientation of the wound was estimated through two proposed functionals of a trace transform. The trace transform [13] is a generalized version of the Radon transform, which scans an image with a series of lines or traces defined by two parameters: an orientation φ and a radius ρ , relative to an origin O . The transform then calculates a functional Tr over the trace t defined by (φ, ρ) . The Radon transform is obtained with an integral or sum as the functional. The Trace transform results in a 2D function of the variables (φ, ρ) . With the use of

two more functionals, *diametrical P*, and *circus Φ*, over each of the variables, a single number called the *triple feature* can be obtained: $\Phi[P[T_r[I]]]$. For this

work we propose to use $Tr = \frac{1}{N} \sum_{i=0}^N t_i$ and $P = std(T_r[I])$ as functionals to

calculate the wound orientation, with the idea that traces perpendicular to the wound will present a relatively uniform average intensity compared to those parallel to the wound, as some of these will trace over the wound itself and others over the cellular regions. The structural element was generated as a dilated line with the orientation previously calculated. The morphological operations aimed first to consolidate the regions with cells by performing a *closing* operation and then filling holes, and then to clear the region of the wound by two *opening* operations; with the structural element and its 90° orthogonal projection.

The principle behind the morphological operators was to consolidate the cellular regions and the wound by removing those details of the image (holes and spots) smaller than the structuring element. The edges of the cellular regions together with other artefacts in the image were obtained by zero crossing. The length of all edges was calculated, and the two longest edges were considered as the boundaries of the cellular regions and the wound. Finally, for each point in a boundary, the distances to all the points in the opposite boundary were calculated and the minimum of this set was selected and assigned to that point. The average distance between the boundaries was the mean of the distances assigned to each point in both boundaries.

The results were validated manually. For each image, the boundaries were estimated visually and 5 distance measurements were hand-traced using

ImageJ (National Institute of Mental Health, Bethesda, Maryland, USA). The mean value of the 5 measurements (d_m) was compared with the previously estimated average distance (d_a) as the following error rate $(d_m - d_a) / d_a$.

Results:

The algorithm was tested on 23 preparations imaged at two time points, one at the time of the scratch and another one 6 hours later. For the 46 images the algorithm calculated correctly the boundaries of the regions.

Figure 1 (top left) shows one representative image of a scratch wound assay at time $t = 0$, h. The wound appears as an empty region in the centre. The square denotes a detail of the image that is shown on the top right. Certain characteristics of the image should be noted: first, the cells are relatively sparse and not too clumped, second, the scratch wound region contains many visual artefacts and last, the intensity of the image is not homogeneous; there are darker and brighter regions. The middle left presents the high pass filtered image with its thresholded image on the right. The result of closing and opening and the corresponding boundaries (dilated for visual purposes) are presented on the bottom images.

Figure 2 presents the results corresponding to $t = 0$, h (top) and $t = 6$, h (bottom). The boundaries between the cells and the wound are labelled with thick white lines. A thick grey line with circular markers lines represents the shortest distance between boundaries, two thin black lines represent a straight-line approximation of the boundaries, and the intensity of the pixels corresponding to the wound has been darkened. The results for these images are: minimum distance = 578.7, pixels, average distance = 624, pixels, relative area of the wound = 49.9% at $t = 0$, h, and minimum distance = 495.2,

pixels, average distance = 538, pixels, relative area of the wound = 43.2% at $t = 6$, h. The error rates for figure 2 were 1.26% and 1.07% respectively and the average for the 46 images was 4.12%.

Conclusion:

The algorithm accurately detected cellular regions in the scratch wound assays through the spatial variation of high frequencies in the images and consolidated the boundaries through mathematical morphology. The algorithm can be run as a background process on a batch of images, it does not require user intervention, a second fluorescent image, the wound to be oriented at a certain angle or the cells to be tightly packed. Since the average distance is calculated from all the points in the boundaries, small curves or variations on the boundaries do not have a significant impact on the average value. As an indication of the computational complexity, the average time to process a 960 x 1280 image was 70 s (Matlab version 6.5 R13 running on a Mac PowerBook G4 OS X 10.3.9).

Acknowledgements

This work was funded by Cancer Research UK.

References

- [1] L. G. Rodriguez, X. Wu, and J. L. Guan, "Wound-healing assay," *Methods Mol Biol*, vol. 294, pp. 23-9, 2005.
- [2] C. R. Keese, J. Wegener, S. R. Walker, and I. Giaever, "Electrical wound-healing assay for cells in vitro," *Proc Natl Acad Sci U S A*, vol. 101, pp. 1554-9, 2004.
- [3] K. A. Pinco, W. He, and J. T. Yang, "alpha4beta1 integrin regulates lamellipodia protrusion via a focal complex/focal adhesion-independent mechanism," *Mol Biol Cell*, vol. 13, pp. 3203-17, 2002.

- [4] J. Wegener, C. R. Keese, and I. Giaever, "Recovery of adherent cells after in situ electroporation monitored electrically," *Biotechniques*, vol. 33, pp. 348, 350, 352 passim, 2002.
- [5] Z. Kornyei, A. Czirok, T. Vicsek, and E. Madarasz, "Proliferative and migratory responses of astrocytes to in vitro injury," *J Neurosci Res*, vol. 61, pp. 421-9, 2000.
- [6] S. Blacher, M. Jost, L. Melen-Lamalle, L. R. Lund, J. Romer, J. M. Foidart, and A. Noel, "Quantification of in vivo tumor invasion and vascularization by computerized image analysis," *Microvasc Res*, 2007.
- [7] J. Qin, T. W. Chittenden, L. Gao, and J. D. Pearlman, "Automated migration analysis based on cell texture: method & reliability," *BMC Cell Biol*, vol. 6, pp. 9, 2005.
- [8] A. Boucher, A. Doisy, X. Ronot, and C. Garbay, "Cell Migration Analysis after *In-Vitro* Wounding Injury with a Multi-Agent Approach," *Artif Intell Rev*, vol. 12, pp. 137-162, 1998.
- [9] J. C. Yarrow, Z. E. Perlman, N. J. Westwood, and T. J. Mitchison, "A high-throughput cell migration assay using scratch wound healing, a comparison of image-based readout methods," *BMC Biotechnol*, vol. 4, pp. 21, 2004.
- [10] H. Samet, "The Quadtree and Related Hierarchical Data Structures," *Computing Surveys*, vol. 16, pp. 187-260, 1984.
- [11] N. Otsu, "A Threshold selection method from gray level histograms," *IEEE Trans on Systems, Man and Cybernetics*, vol. 9, pp. 62-66, 1979.
- [12] G. Matheron, *Random Sets and Integral Geometry*. New York: Wiley, 1975.
- [13] A. Kadyrov and M. Petrou, "The Trace Transform and its Applications," *IEEE Trans on Patt Anal and Machine Intell*, vol. 23, pp. 811-828, 2001.

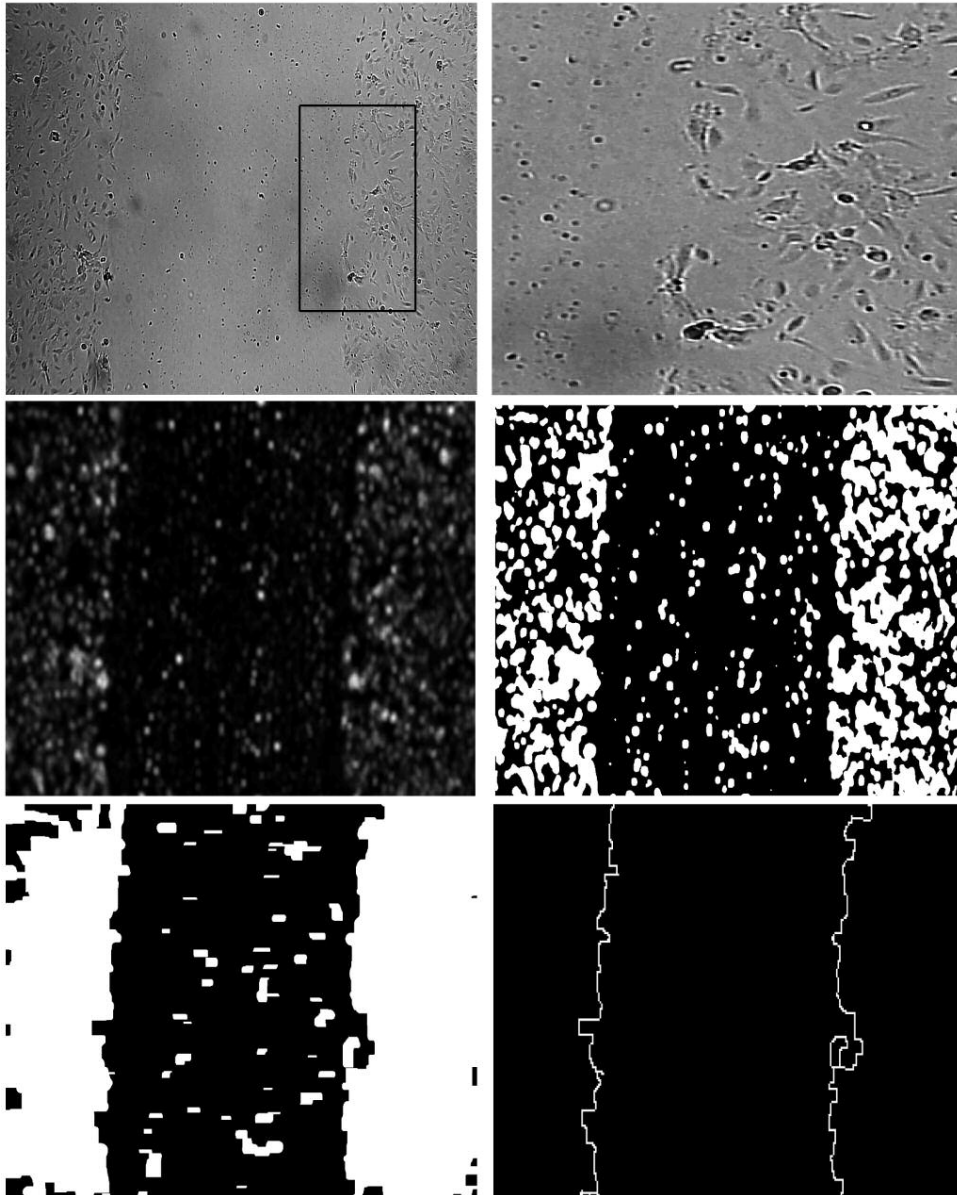
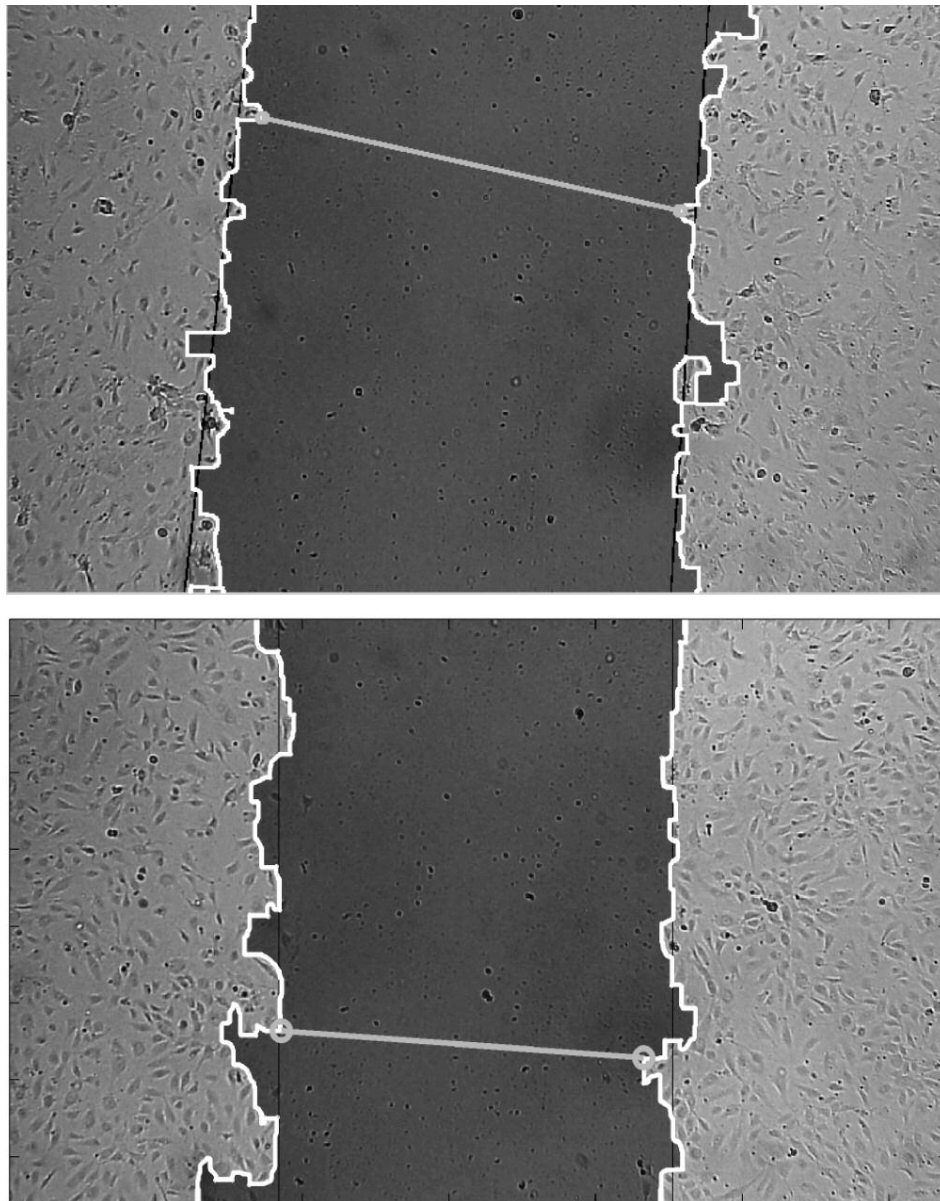


Image-processing algorithm to approximate the boundaries of a scratch wound assay. Top row: a representative image at time $t = 0$, h. The square denotes a detail of the image that is shown on the right. Middle row: high pass filtered image and binary image produced by thresholding. Bottom row: result of morphological closing and opening and the boundaries (dilated for visual purposes) corresponding to the two longest edges.



Labelled scratch wound assay at times $t = 0, 6, h$. The boundaries between cellular regions and the wound are labelled with thick white lines. A thick grey line with circular markers represents the shortest distance between boundaries, two thin black lines represent a straight-line approximation of the boundaries, and the intensity of the pixels corresponding to the wound has been darkened. Distances: minimum = 578.7, 495.2, average = 624, 538, pixels, relative area of the wound = 49.9, 43.2, %.